https://doi.org/10.1016/j.ijheatmasstransfer.2019.02.059

Measuring thermal conductivity of ultra-small materials exampled by the reaction chambers of bombardier beetles

Zhenbin Guo, Wenhao Sha, Haimin Yao*

Department of Mechanical Engineering, The Hong Kong Polytechnic University,

Hung Hom, Kowloon, Hong Kong, China

Abstract

Bombardier beetles, as their name implies, defend themselves against the potential predators by spraying boiling-hot and corrosive chemicals which are products of an explosive biochemical reaction taking place in the paired organs called reaction chambers (RCs). Why these beetles can withstand the explosive reaction that takes place in their bodies? Knowledge of thermal properties of the RCs will help to shed light on this puzzle. However, the submillimeter dimension and irregular shape of the RCs discourage the traditional methods for thermal characterization. To overcome this challenge, in this paper a method is developed particularly for measuring the thermal conductivity of a material with dimension as small as submillimeter. The measurement results by this method are demonstrated reliable especially for polymeric or organic materials including the RCs of bombardier beetles. The results in this paper not only help to understand the superior thermal insulation of the RC wall but also offer a facile approach to measuring the thermal conductivity of materials in submillimeter scale.

Keywords: thermal conduction, thermal characterization, biomaterials, thermal properties, thermal insulation

* To whom correspondence should be addressed, E-Mail: mmhyao@polyu.edu.hk

1. Introduction

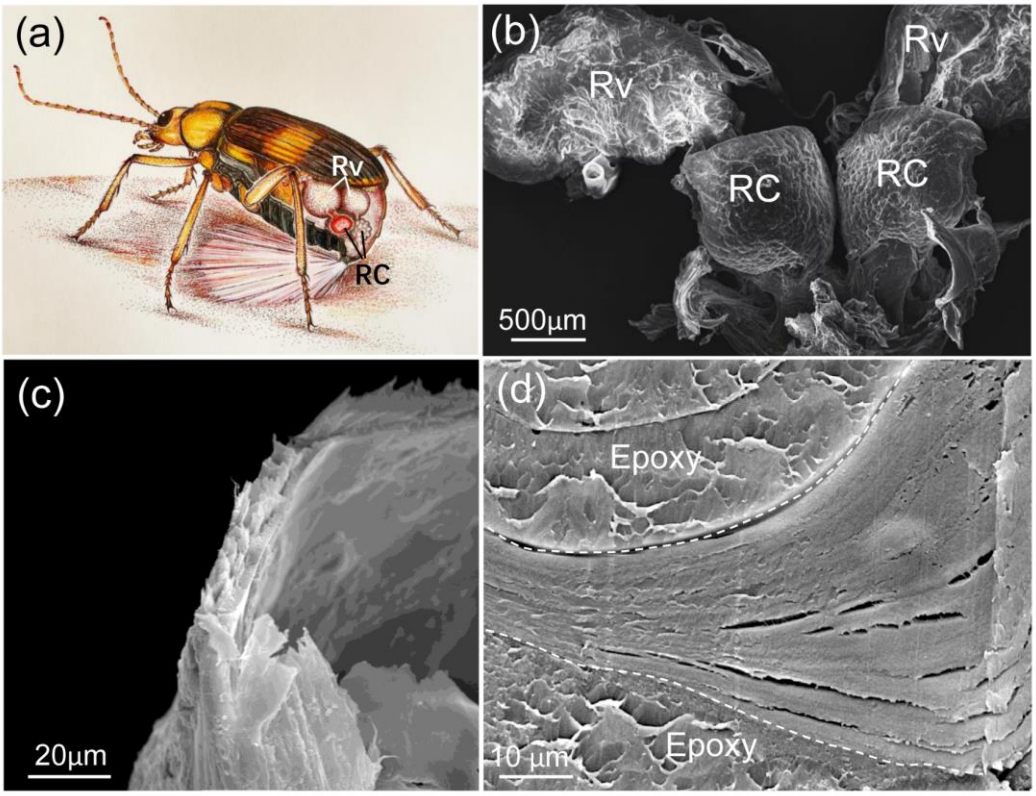

Figure 1. (a) Schematics of a bombardier beetle, SEM images of (b) reaction chambers, (c) wall of a RC, and (d) cross section of the wall of a RC embedded in epoxy. Rv: reservoir; Gl: gland; RC: reaction chamber. Illustration courtesy of Jing Xiao from Guangzhou Academy of Fine Arts.

Rarely has a beetle been named as aptly as the bombardier beetle which ejects hot and corrosive spray as a defensive mechanism against the would-be predators [1, 2]. The spray is the product of a chemical reaction between hydroquinone and hydrogen peroxide which are gland secretions usually stored in a pair of reservoirs in the peaceful time (**Figure 1a**). Each reservoir is connected to a reaction chamber (RC) through a one-way valve. When the beetle encounters threat, the valves are opened and the reactants flow into the RCs where they meet enzymes catalases and peroxidases. Reaction thus takes place instantly and oxygen is liberated from the hydrogen peroxide. The hydroquinone is oxidized by the freed oxygen which also serves as propellant to push the reaction products out through spray nozzles. As the whole process is heat-

producing, the temperature of the resultant spray can reach as high as 100 ℃ [3-5]. How do the RCs withstand such high temperature during defense? How are the tissues and organs outside the RCs protected from being overheated? Knowledge of the material compositions and thermal properties of the RCs helps to shed light on these questions.

2. Material characterization

Figure 1b shows the Scanning Electron Microscopy image of the RCs, which are hollow sacs with characteristic size less than 1 mm and wall thickness around 10 micrometers on average (**Figure 1c, d**). To characterize the material composition of the RCs, thermogravimetric analysis (TGA) and the X-ray diffraction (XRD) analysis were carried out to characterize the material compositions of the RC.

2.1 The thermogravimetric analysis

For TGA, more than eighty RCs were dissected from the bombardier beetles (*Pheropsophus verticalis*) with the aid of optical microscope. The RCs were then milled into powder with pestle and mortar. A sieve was used to spread the powder sample evenly on the bottom of the sample holder for TGA. Thermogravimetric analysis (TGA/DSC 3+, Mettler Toledo) was carried out at a heating rate of 5 °C/min in air. A four-step weight loss process was observed, as shown in **Figure 2a**. In the first step from 25 to 120 °C, weight loss of ~7.95% was observed, which is mainly due to the removal of adsorbed water and moisture in the sample. In the subsequent second step up to 234˚C, decomposition of the material started, resulting in another weight loss of ~12.56 wt%. The most significant weight loss of ~47.72% happened in the third step at temperatures up to 424 °C owing to the evaporation of the organic components. The fourth major weight loss (~29.49%) occurred at temperatures up to 620 °C. The final ~2.28% residual was most probably inorganic materials. Thermogravimetric analysis

shows that the RCs contains ~7.95 wt% water, ~89.77 wt% organic materials and ~2.28 wt% inorganic materials.

2.2 The X-ray Diffraction Analysis

For XRD analysis, sufficient RCs were dissected from bombardier bettles, rinsed thoroughly with DI water and then freeze-dried at $-50^{\circ}C$ for 8 h (FD-1A-50 Freeze Dyer, Shanghai Bilon Instrument). The samples were then milled into powder with pestle and mortar. A sieve was used to mount the powder sample into the sample holder evenly. XRD analysis was performed on a Rigaku-Smartlab diffractometer using Cu K_α radiation (wavelength $\lambda = 0.154$ nm). As shown in **Figure 2b**, the four diffraction peaks observed at $2\theta = 9.3°$, 19.3°, 20.9°, and 26.6° corresponds to (020), (110), (120), and (003) planes of chitin respectively [6]. Therefore, it can be concluded from the X-ray diffraction analysis that the organic composition in RCs is mainly chitin, which is also the main building material of the arthropod exoskeletons such as shrimp shells. Although there are many technologies for measuring the thermal conductivities of materials such as the steady-state method, 3ω technique and transient hot-strip technique [7-10], they all fall short when measuring RCs with such small size and irregular shape. To characterize the thermal conductivity of the wall of RCs, it is necessary to develop a new method applicable to materials with dimension as small as submillimeter.

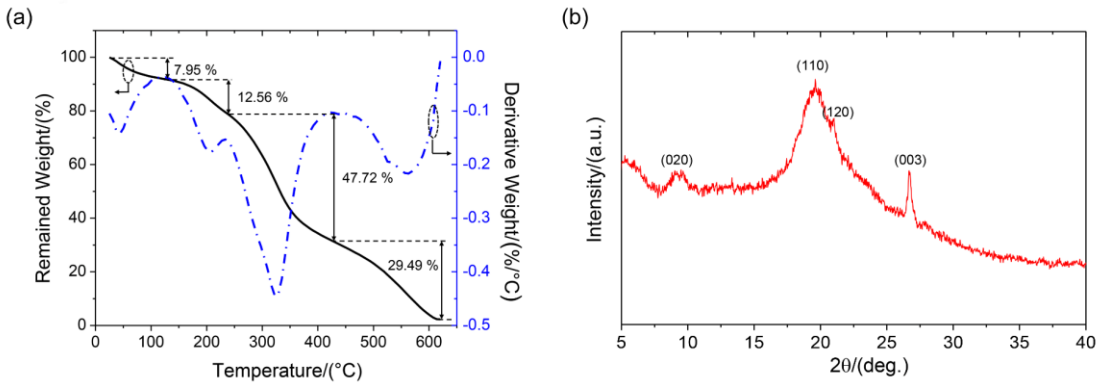

Figure 2. (a) Thermogravimetric analysis result of the RCs of bombardier beetles. (b) X-ray diffraction pattern acquired from powder sample of RCs. Diffraction peaks observed at $2\theta = 9.3°$, 19.5°, 20.9°, and 26.6°, which agree well with the characteristic peaks of chitin at $2\theta = 9.2233°$, 19.3093°, 20.8119°, and 26.4454° as reported [6].

3. Theoretical formulation

Thermal conductivity describes material's competence to conduct heat. The speed of heat transfer in a material is significantly affected by its thermal conductivity, implying that the thermal conductivity of a material could be deduced from the measured rate of heat transfer if the relationship between them is known. Inspired by this conception, here we consider a one-dimensional thermal conduction problem, in which a material sample of thickness d is in attached to a reference material with infinite dimension along x-direction (see **Figure 3a**). Initially, the temperature of the whole system is uniform and equal to T_0. At time $t = 0$, the temperature at the end of the sample ($x = -d$) is instantly increased to T_f and kept at this value all along. Due to the heat transfer in the sample, the temperature in the sample increases. The increasing rate at a specific position, such as the interface between the sample and reference material ($x = 0$), depends on the thermal conductivity of the sample. In the following, theoretical analysis will be carried out to reveal the dependence.

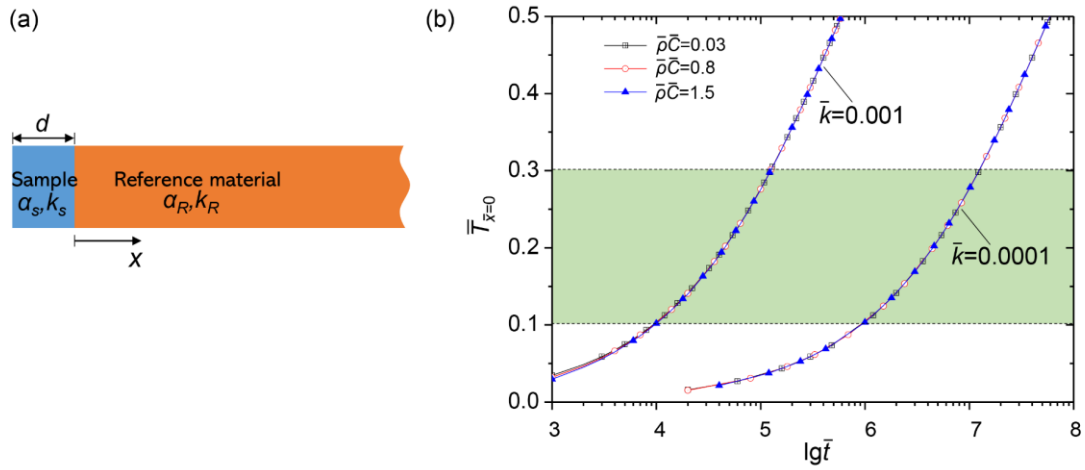

Figure 3. (a) Schematic depiction of 1-D thermal conduction model of a composite consisting of a plate (sample) attached on a semi-infinite reference material. (b) Evolution of the normalized temperature at the interface (x =0) with the normalized time for cases with different values of normalized volumetric heat capacity $\bar{\rho}\bar{C}$ and normalized thermal conductivities $\bar{k}$.

As there is no internal heating source, the evolution of temperature field $T(x, t)$ in the whole system should satisfy following governing equations

$$\begin{cases} \dfrac{\partial T}{\partial t} = \alpha_s \dfrac{\partial^2 T}{\partial x^2}, & (-d \le x < 0) \\ \dfrac{\partial T}{\partial t} = \alpha_R \dfrac{\partial^2 T}{\partial x^2}, & (x > 0) \end{cases} \tag{1}$$

where $\alpha_s = \dfrac{k_s}{\rho_s C_p^s}$ and $\alpha_R = \dfrac{k_R}{\rho_R C_p^R}$ are the thermal diffusivities of the sample and the reference material, respectively with $k_{s/R}$, $\rho_{s/R}$, $C_p^{s/R}$ being the thermal conductivity, density and thermal capacity of the sample (s) or reference materials (R), respectively. Introduce nondimensional parameters $\bar{T} = \dfrac{T - T_0}{T_f - T_0}$, $\bar{x} = x/d$, $\bar{t} = \dfrac{\alpha_R t}{d^2}$, $\bar{\alpha} = \alpha_s / \alpha_R$. Eq. (1) can be further normalized to be

$$\begin{cases} \dfrac{\partial \bar{T}}{\partial \bar{t}} = \bar{\alpha}\dfrac{\partial^2 \bar{T}}{\partial \bar{x}^2}, & \left(-1 \le \bar{x} \le 0\right) \\ \dfrac{\partial \bar{T}}{\partial \bar{t}} = \dfrac{\partial^2 \bar{T}}{\partial \bar{x}^2}, & \left(\bar{x} \ge 0\right) \end{cases} \tag{2}$$

The boundary conditions and the initial condition can be written as

$$\bar{T}(-1,\bar{t}) = 1, \bar{T}(\infty,\bar{t}) = 0, \bar{T}(\bar{x},0) = 0 \ \left(\bar{x} \ge -1\right). \tag{3}$$

Moreover, on the interface ($\bar{x} = 0$) between the sample and the reference material, the conservation of thermal flux and continuity of temperature require

$$\bar{k}\frac{\partial \bar{T}(0^-,\bar{t})}{\partial x} = \frac{\partial \bar{T}(0^+,\bar{t})}{\partial x}), \ \ \bar{T}(0^-,\bar{t}) = \bar{T}(0^+,\bar{t}), \tag{4}$$

where $\bar{k} = k_s / k_R$. The solution to the above thermal conduction problem is given by [11, 12]

$$\begin{cases} \bar{T}(\bar{x},\bar{t}) = \sum_{n=0}^{\infty} \beta^n \left\{ \mathrm{erfc}\left[\dfrac{(2n+1)+\bar{x}}{2\sqrt{\bar{\alpha}\bar{t}}}\right] - \beta \cdot \mathrm{erfc}\left[\dfrac{(2n+1)-\bar{x}}{2\sqrt{\bar{\alpha}\bar{t}}}\right] \right\}, & \left(-1 < \bar{x} < 0\right) \\ \bar{T}(\bar{x},\bar{t}) = (1-\beta)\sum_{n=0}^{\infty} \beta^n \cdot \mathrm{erfc}\left[\dfrac{(2n+1)+\bar{x}\sqrt{\bar{\alpha}}}{2\sqrt{\bar{\alpha}\bar{t}}}\right], & \left(\bar{x} > 0\right) \end{cases} \tag{5}$$

where $\beta = \dfrac{\sqrt{\bar{\alpha}} - \bar{k}}{\sqrt{\bar{\alpha}} + \bar{k}}$. The evolution of temperature at the interface ($\bar{x} = 0$) thus is given by

$$\bar{T}_{|\bar{x}=0}(\bar{t}) = (1-\beta)\sum_{n=0}^{\infty} \beta^n \cdot \mathrm{erfc}\left[\frac{(2n+1)}{2\sqrt{\bar{\alpha}\bar{t}}}\right]. \tag{6}$$

Considering $\bar{\alpha} = \dfrac{\alpha_s}{\alpha_R} = \dfrac{k_s}{\rho_s C_s}\dfrac{\rho_R C_R}{k_R}$ and $\beta = \dfrac{\sqrt{\bar{\alpha}} - \bar{k}}{\sqrt{\bar{\alpha}} + \bar{k}}$, Eq. (6) implies that the evolution of the temperature at the interface depends on the normalized thermal conductivity $\bar{k}$ and the normalized volumetric heat capacity $\bar{\rho}\bar{C}$, where $\bar{\rho} = \rho_s / \rho_R$ and $\bar{C} = C_s / C_R$.

Taking copper as the reference material with $k_R = 398\ \mathrm{W/m \cdot K}$, $C_R = 390\ \mathrm{J/kg \cdot K}$ and $\rho_R = 8.96 \times 10^3\ \mathrm{kg/m^3}$, the normalized volumetric heat capacity $\bar{\rho}\bar{C}$ and the normalized thermal conductivity $\bar{k}$ of typical polymers, ceramics and metals are shown in an Ashby diagram (see **Figure 4)**. By and large, both $\bar{\rho}\bar{C}$ and $\bar{k}$ exhibit descending trend from metals through ceramic to polymers. In **Figure 4**, the largest values of $\bar{\rho}\bar{C}$ and $\bar{k}$ occur in the metal regime and take around 1.5 and 1.0, respectively. In contrast, $\bar{\rho}\bar{C}$ and $\bar{k}$ of polymeric materials are distributed in the lower ranges of 0.03-0.8 and 10^{-4}-10^{-3}, respectively. Therefore, for the RC, which is a chitin-rich composite, the normalized thermal conductivity $\bar{k}$ is believed to range from 10^{-4} to 10^{-3}.

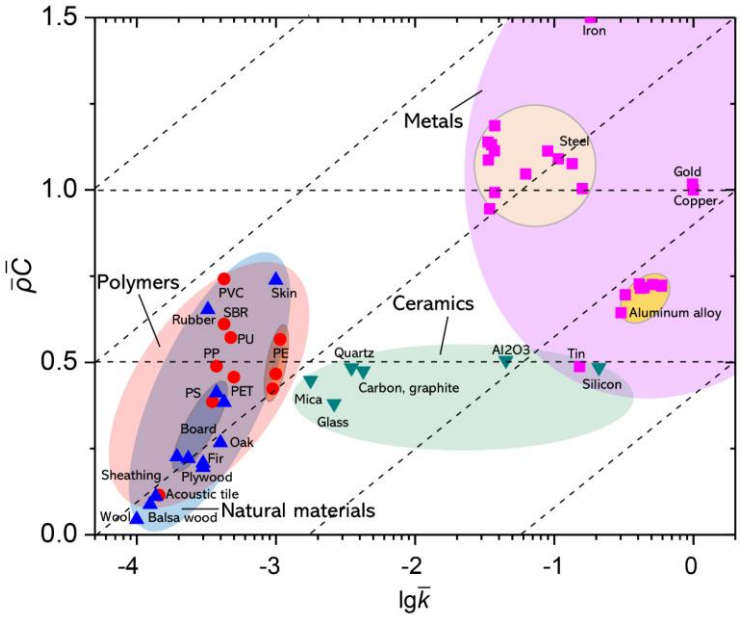

Figure 4. Ashby diagram of thermal conductivity versus volumetric heat capacity, where all the values are normalized by the properties of copper[13-19].

Taking $\bar{k} = 10^{-4}$ and 10^{-3}, **Figure 3b** shows the evolution of the temperature at the interface (x=0) for $\bar{\rho}\bar{C}$ = 0.03, 0.8 and 1.5 (the upper bound in **Figure 4**),

respectively. It can be seen that the evolution of temperature $\bar{T}_{\bar{x}=0}$ depends little on $\bar{\rho}\bar{C}$ but is sensitive to $\bar{k}$, implying that $\bar{k}$ can be deduced from the evolution of temperature without knowledge of $\bar{\rho}\bar{C}$. To delineate the evolution of temperature, we examine the time ($\Delta\bar{t}_{\bar{T}_1\to\bar{T}_2}$) needed for $\bar{T}_{\bar{x}=0}$ to increase from one prescribed temperature $\bar{T}_1$ to another $\bar{T}_2$. For example, $\Delta\bar{t}_{0.1\to0.3}$, which represents the time for $\bar{T}_{\bar{x}=0}$ increasing from $\bar{T}_1=0.1$ to $\bar{T}_2=0.3$, can be determined by solving Eq. (6) with $\bar{T}_{\bar{x}=0}$ being taken as 0.1 and 0.3 respectively. **Figure 5** shows $\Delta\bar{t}_{0.1\to0.3}$ as a function of $\bar{k}$ for $\bar{\rho}\bar{C}=0.03$, 0.8 and 1.5. As expected, $\Delta\bar{t}_{0.1\to0.3}$ is insensitive to $\bar{\rho}\bar{C}$ especially when $\bar{k}$ is less than a critical value. If we take <5% deviation between the curves in **Figure 5** as the threshold of insensitivity of $\Delta\bar{t}_{0.1\to0.3}$ to $\bar{\rho}\bar{C}$, such critical $\bar{k}$ is estimated to be around 0.03 from **Figure 5**. For all the organic materials and most ceramic materials, $\bar{k}$ is less than 0.03, as shown in **Figure 4**. Therefore, the normalized thermal conductivity $\bar{k}$ of RC, which is mainly composed of chitin, can still be deduced from $\Delta\bar{t}_{0.1\to0.3}$ even though its $\bar{\rho}\bar{C}$ is unknown. However, for materials with $\bar{k}>0.03$, determination of $\bar{k}$ needs the prior knowledge of $\bar{\rho}\bar{C}$. If $\bar{\rho}\bar{C}$ is unknown, estimation of a reasonable range of $\bar{k}$ can still be made based on the estimation of the lower and upper bounds of $\bar{\rho}\bar{C}$. In this sense, reference material with high thermal conductivity is preferred as it results in lower $\bar{k}$ and therefore less dependence of $\Delta\bar{t}_{0.1\to0.3}$ on $\bar{\rho}\bar{C}$ as shown in **Figure 5**. That's why copper is taken as the reference material in the ensuing experimental implementation. After determining the $\bar{k}$ of the sample, the real thermal conductivity is obtained by multiplying $\bar{k}$ by the thermal

conductivity of the reference material. Therefore, high thermal conductivity of the reference material may lead to large absolute error of the measured thermal conductivity of the sample. For a measurement requiring higher precision, proper reference material should be selected.

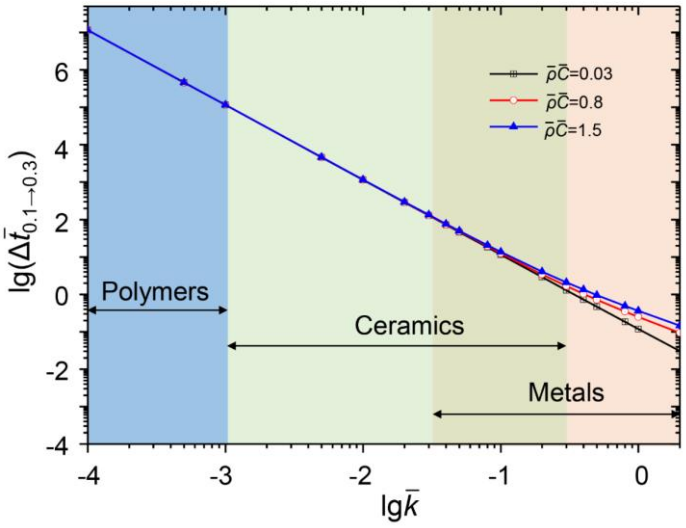

Figure 5. The time needed for the temperature at $x = 0$ to increase from $\bar{T}_1 = 0.1$ to $\bar{T}_2 = 0.3$ as a function of $\bar{k}$ for $\bar{\rho}\bar{C}$ =0.03, 0.8 and 1.5.

4. Experimental implementation

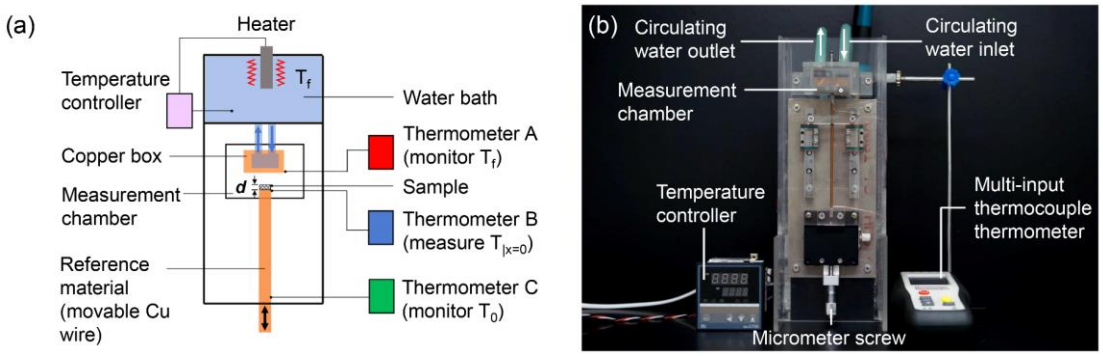

Figure 6. (a) Schematic depiction and (b) photo of an apparatus for measuring the thermal conductivity. Here, K-type thermocouple thermometers (YHT309, Yuan Hengtong Technology Co., Ltd) with 1 °C accuracy are used.

Based on the results of theoretical modeling above, an experimental apparatus is developed, as shown in **Figure 6**. Here, a copper wire with diameter of 1.2 mm is taken as the reference material. A copper box (externally 40 mm×40 mm×10 mm) with

constant temperature (T_f) maintained by circulating hot water serves as a constant temperature source. Take $T_0 = 25^\circ\mathrm{C}$, $T_f = 75^\circ\mathrm{C}$, $T_1 = 30^\circ\mathrm{C}$ and $T_2 = 40^\circ\mathrm{C}$, we have $\bar{T}_1 = 0.1$ and $\bar{T}_2 = 0.3$. To verify the applicability of our method, measurements are first carried out on two benchmark samples. **Table 1** shows the measured results obtained in comparison to those acquired by a commercial tester (Flashline 2000, Thermal Properties Analyser). The small difference between the results obtained by our apparatus and the commercial tester confirms the reliability of the measurements by this apparatus. Admittedly, slight underestimate is observed in our results compared to those given by the commercial tester. This may be attributed to the imperfectly adiabatic condition in our measurement and the possible size inconformity between the sample and reference material. Another possible factor causing the underestimate is the thermal contact resistance due to the imperfect contact between the sample and heat source (copper box) as well as the reference material (copper wire), although slight compression has been applied on the samples to reduce this effect by the micrometer screw (see **Figure 6b**) during the measurement. Moreover, application of thermocouples with rapider response and higher precision is believed to improve the accuracy of the measurements.

Table 1. Measurement results of benchmark samples

Material	Sample thickness *d*	Thermal Conductivity (Flashline 2000)	Thermal Conductivity (this work)
Carbon fiber-reinforced composite	1.1 mm	1.90 W/m·K ($\bar{k} = 4.77\times10^{-3}$)†	1.74 W/m· K ($\bar{k} = 4.37\times10^{-3}$)†
310 Stainless Steel	1.0 mm	11.3 W/m·K ($\bar{k} = 2.84\times10^{-2}$)†	9.95 W/m·K ($\bar{k} = 2.50\times10^{-2}$)†

† $\bar{k}$ is the thermal conductivity normalized by the value of copper.

To further measure the thermal conductivity of the RCs, we prepare disk-like samples dissected from the wall of RCs with the aid of an optical microscope. The diameter of the sample is 1.2 mm and the thickness ranges from 17 to 24 μm as measured through SEM imaging. By using the apparatus developed above, the thermal

conductivity of the RC is measured to be $(3.31\pm1.29)\times10^{-2}$ W/m·K.

5. Discussion and conclusion

In this paper, a new experimental method is developed to measure the thermal conductivity of the RCs of bombardier beetles. The measurement results indicate that the RCs exhibit thermal conductivity as low as $(3.31\pm1.29)\times10^{-2}$ W/m·K. This value, if converted into the normalized value as we defined above, is equal to $\bar{k}=(8.30\pm3.20)\times10^{-5}$, which is below the lower limit of the thermal conductivities of all the materials shown in **Figure 4** and even comparable to those of the insulation materials applied in engineering [20]. It is such low thermal conductivity that endows the RCs with superior thermal insulation, protecting the tissues and organs outside from being overheated. Clearly, such low thermal conductivity of RCs is not the characteristics of chitin because shrimp shell, which is also composed of chitin, is found to have thermal conductivity $(1.03\pm0.175)\times10^{-1}$ W/m·K, which is more than three times of the RCs'. The cause of the ultralow thermal conductivity of RCs may lie in the laminar and porous structures of the wall (**Figure 1d**). Investigation of the relationship between thermal properties and microscopic structures of RCs is beyond the scope of this paper and leaves to our future work.

Conflict of interest

The authors declare that there is no conflict of interest.

Acknowledgements

This work is supported by the Departmental General Research Fund of The Hong Kong Polytechnic University (G-UB51).

References

[1] T. Eisner, J. Meinwald, Defensive Secretions of Arthropods, Science 153 (1966) 1341-1350.
[2] D.J. Aneshans, T. Eisner, J.M. Widom, B. Widom, Biochemistry at 100 degrees C: Explosive Secretory Discharge of Bombardier Beetles (Brachinus), Science 165 (1969) 61-63.
[3] J. Dean, D.J. Aneshansley, H.E. Edgerton, T. Eisner, Defensive spray of the bombardier beetle: a biological pulse jet, Science 248(4960) (1990) 1219-1221.
[4] T. Eisner, D.J. Aneshansley, J. Yack, A.B. Attygalle, M. Eisner, Spray mechanism of crepidogastrine bombardier beetles (Carabidae; Crepidogastrini), Chemoecology 11(4) (2001) 209-219.
[5] E.M. Arndt, W. Moore, W.-K. Lee, C. Ortiz, Mechanistic origins of bombardier beetle (Brachinini) explosion-induced defensive spray pulsation, Science 348(6234) (2015) 563-567.
[6] A. Raut, R. Satvekar, S. Rohiwal, A. Tiwari, A. Gnanamani, S. Pushpavanam, S. Nanaware, S. Pawar, In vitro biocompatibility and antimicrobial activity of chitin monomer obtain from hollow fiber membrane, Designed Monomers and Polymers 19(5) (2016) 445-455.
[7] J.C. Lambropoulos, M. Jolly, C. Amsden, S. Gilman, M. Sinicropi, D. Diakomihalis, S. Jacobs, Thermal conductivity of dielectric thin films, Journal of Applied Physics 66(9) (1989) 4230-4242.
[8] T. Borca-Tasciuc, A. Kumar, G. Chen, Data reduction in 3ω method for thin-film thermal conductivity determination, Review of Scientific Instruments 72(4) (2001) 2139-2147.
[9] S.E. Gustafsson, E. Karawacki, M.N. Khan, Transient hot-strip method for simultaneously measuring thermal conductivity and thermal diffusivity of solids and fluids, Journal of Physics D: Applied Physics 12(9) (1979) 1411.
[10] S. Perichon, V. Lysenko, P. Roussel, B. Remaki, B. Champagnon, D. Barbier, P. Pinard, Technology and micro-Raman characterization of thick meso-porous silicon layers for thermal effect microsystems, Sensors and Actuators A: Physical 85(1-3) (2000) 335-339.
[11] A.V. Luikov, Analytical heat diffusion theory, Academic Press, New York, 2012.
[12] V.S. Arpaci, Conduction heat transfer, Addison-Wesley Pub. Co., Reading, MA, 1966.

[13] M. Janssens, Cone calorimeter measurements of the heat of gasification of wood, in: Proceedings of Interflam, Interscience Communications, 1993, pp. 549-558.
[14] D. Hopkins Jr, J.G. Quintiere, Material fire properties and predictions for thermoplastics, Fire Safety Journal 26(3) (1996) 241-268.
[15] A. Tewarson, Generation of heat and chemical compounds in fires, in: P.J. DiNenno (Ed.) SFPE handbook of fire protection engineering, National Fire Protection Association, Quincy, MA, 2002.
[16] T.L. Bergman, F.P. Incropera, D.P. DeWitt, A.S. Lavine, Fundamentals of heat and mass transfer, John Wiley & Sons, Hoboken, NJ, 2011.
[17] M.J. Spearpoint, J.G. Quintiere, Predicting the piloted ignition of wood in the cone calorimeter using an integral model—effect of species, grain orientation and heat flux, Fire Safety Journal 36(4) (2001) 391-415.
[18] H.C. Tran, R.H. White, Burning rate of solid wood measured in a heat release rate calorimeter, Fire and Materials 16(4) (1992) 197-206.
[19] R.J. Ross, Wood handbook: wood as an engineering material, in: General Technical Report FPL-GTR-190, USDA Forest Service, Forest Products Laboratory, Mandison, Wisconsin, 2010.
[20] I. Budaiwi, A. Abdou, M. Al-Homoud, Variations of thermal conductivity of insulation materials under different operating temperatures: Impact on envelope-induced cooling load, Journal of architectural engineering 8(4) (2002) 125-132.